The mechanism of the rutile-to-$CaCl_2$ phase transition: RuO_2 and β-PtO_2

2000 J. Phys.: Condens. Matter 12 6725

(http://iopscience.iop.org/0953-8984/12/30/305)

J. Phys.: Condens. Matter **12** (2000) 6725–6734. Printed in the UK PII: S0953-8984(00)09376-0

The mechanism of the rutile-to-$CaCl_2$ phase transition: RuO_2 and β-PtO_2

Ruqian Wu† and W H Weber‡

† Department of Physics and Astronomy, California State University, Northridge, CA 91330-8268, USA

‡ Physics Department, MD3028, Ford Research Laboratory, Ford Motor Company, Dearborn, MI 48121-2053, USA

Received 8 November 1999

Abstract. Using the full-potential linearized augmented-plane-wave (FLAPW) method, the mechanism of the rutile–$CaCl_2$ phase transition of RuO_2 and the phase stability of β-PtO_2 are investigated. The local density functional calculations predict quantities such as lattice constants, bulk moduli, and phonon frequencies in good agreement with experiment. The pressure-induced phase transition in RuO_2 appears to be driven by the strong repulsion between O–O and Ru–O along the diagonal direction in the xy-plane. By contrast, a strong hybridization between the Pt 5d and O 2p states is responsible for the stability of the β-PtO_2 structure, for which a pseudo-gap (instead of the strong peak for the rutile-PtO_2) is opened at the Fermi level due to the rotation of the PtO_6 octahedra.

1. Introduction

Due to its low resistivity and reactivity, RuO_2 is important in industrial applications as a stripline conductor in integrated circuits, as a diffusion barrier in contact metallization, as a catalytic agent, and as a possible electrode material in high-energy-density storage capacitors [1–3]. Under ambient conditions RuO_2 adopts a rutile structure, but under high-pressure conditions it will transform to a denser $CaCl_2$ structure [4, 5]. Since it is isostructural with stishovite (SiO_2), a geologically important mineral that undergoes the same transformation, RuO_2 and other metal dioxides, e.g., SnO_2, PbO_2, and MnO_2, are also interesting model systems for the post-stishovite, high-pressure phases of SiO_2 [6].

The rutile-to-$CaCl_2$ structural transformation is a second-order phase transition that occurs, according to the most recent Raman measurements, at a pressure of 11.8 ± 0.3 GPa in RuO_2 [4]. In the rutile structure the metal atoms lie on a body-centred-tetragonal lattice and the oxygens are paired on either side of each cation along (110) directions, for the cations at the corners of the tetragonal unit cell, or $(1\bar{1}0)$ directions, for the body-centred cations. The O–Ru–O bonds thus lie along diagonals in the xy-planes. The phase transition proceeds via a rotation about the c-axis of the distorted RuO_6 octahedra, as shown in figure 1. After the rotation the O–Ru–O bonds make an angle θ with the xy-plane diagonals, and the angle is opposite in sign for the body-centred and corner sites. There is also a small orthorhombic distortion of the lattice that accompanies the rotation of the octahedra. The soft mode that connects the two phases is the B_{1g} mode of rutile, which has A_g symmetry in the $CaCl_2$ structure. We refer to this mode simply as ω_1.

0953-8984/00/306725+10$30.00

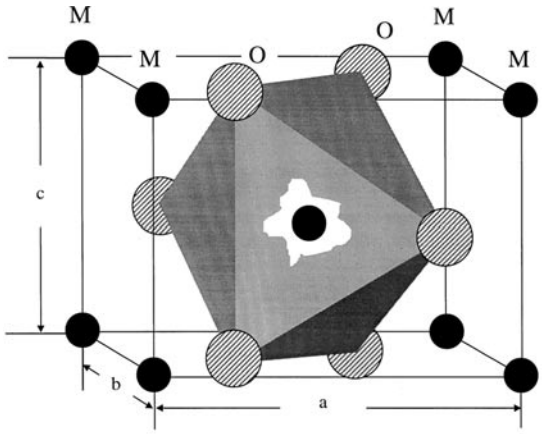

Figure 1. A schematic crystal structure for RuO_2 and β-PtO_2 showing the MO_6 octahedron whose rotation leads to the rutile-to-$CaCl_2$ phase transition.

β-PtO_2 is unique among metal dioxides, in that it has the orthorhombic $CaCl_2$ structure under normal conditions. From the temperature dependence of the ω_1-phonon frequency, however, Weber *et al* [7] showed that β-PtO_2 tends toward the rutile structure as temperature increases, with an extrapolated transition temperature of 1240 K (far above the dissociation limit for the oxide under ambient pressure). The central questions that we address in this paper are (1) what is the driving force for the pressure-induced phase transition for RuO_2 and (2) why does β-PtO_2 crystallize in the $CaCl_2$ structure, whereas most other similar metal dioxides form the rutile structure. Similar first-principles studies of the rutile-to-$CaCl_2$ transition in stishovite have been reported by Karki *et al* [8] and by Lee and Gonze [9]. Although the details differ, both groups find a softening of the rutile B_{1g} phonon mode with increasing pressure and a phase transition to the $CaCl_2$ structure in the 40–60 GPa range, results which are in reasonable agreement with experiment.

Here we report results of first-principles calculations for the structural, mechanical, and electronic properties of RuO_2 and β-PtO_2 using the full-potential linearized augmented-plane-wave (FLAPW) method [10]. We find that the Pt–O interaction is more covalent (via hybridization) whereas the Ru–O interaction is more ionic (charge transfer). The pressure-induced phase transition in RuO_2 appears to be driven by the strong repulsion between O–O and Ru–O along the diagonal direction. By contrast, a strong hybridization between the Pt 5d and O 2p states is responsible for the stability of the β-PtO_2 structure, for which a pseudo-gap (instead of the strong peak for the rutile-PtO_2) is opened at the Fermi level due to the rotation of the PtO_6 octahedra.

2. Methodology and models

As sketched in figure 1, the unit cell for RuO_2 and β-PtO_2 contains two metal atoms and four oxygen atoms. To simplify the calculations and focus on the mechanism of the pressure-induced structural phase transition of RuO_2 and the phase stability of β-PtO_2, we assume a fixed c/a ratio (namely, 0.690 for RuO_2 and 0.694 for β-PtO_2) and ignore the small orthorhombic distortion in β-PtO_2 and RuO_2 in the $CaCl_2$ structure. The first simplification is known to be valid for RuO_2, since the x-ray results of Haines and Léger [5] show that the fractional change with pressure in the c/a ratio for RuO_2 in the rutile-structured region is roughly a

factor of ten smaller than the fractional change in either c or a. There are no corresponding data for β-PtO_2, but it is reasonable to make the same simplifying assumption for that material as well. The small orthorhombic distortion can be ignored, since we are concerned with the *stability* of the rutile structure and the *onset* of the transition to the $CaCl_2$ structure, and both of these questions can be addressed by considering the change in total energy resulting from an infinitesimal rotation of the MO_6 octahedra in a tetragonal (rutile) structure. The total energies are calculated for different fixed values of lattice constants, a, and rotational angles of the MO_6 octahedra, θ. These energies are then minimized with respect to a variable M–O bond length, u (defined as $u = d_{M-O}/a$).

In the FLAPW approach, there is no shape approximation for charge density, wave function, and potential. The single-particle local density functional Kohn–Sham equation (with the Hedin–Lundqvist formula for the exchange–correlation interactions) is solved self-consistently with an energy cut-off of 15 Ryd for the variational augmented-plane-wave basis set. The core electrons are treated fully relativistically, whereas the valence electrons are treated semi-relativistically (without the spin–orbit coupling term). 54 special k-points in the irreducible Brillouin zone are used to evaluate k-space integrals. Within the muffin-tin (MT) spheres ($r_{Ru} = 1.19$ Å, $r_{Pt} = 1.228$ Å, and $r_O = 0.69$ Å), lattice harmonics with a maximum angular momentum l up to 8 are employed to expand the charge density, potential, and wave functions. Convergence is assumed when the root mean square distance between the input and output charge densities is less than 1.0×10^{-4} e au^{-3}.

3. Results

The calculated total energies for RuO_2 are plotted in figure 2 as a function of the lattice expansion (i.e., $a/a_0 - 1$, where $a_0 = 4.51$ Å is the measured lattice constant in the xy-plane) for cases where the O–Ru–O bond is 0°, 3°, and 6° away from the diagonal direction. Clearly, the rutile structure ($\theta = 0°$) has the lowest total-energy minimum and thus should be the ground state under ambient conditions. The calculated equilibrium lattice constants ($a = 4.47$ Å, $c = 3.08$ Å) agree well (within 0.045 Å and 0.031 Å, respectively) with the known parameters [5]. To fit the energy curves with a polynomial in the lattice constant, we need to include at least the cubic term, which indicates that the elastic properties (e.g. bulk moduli and phonon frequencies) depend strongly on the lattice size (or pressure). The calculated bulk modulus is 326 GPa for the structure with the calculated equilibrium lattice constant but changes to 278 GPa for that with the measured lattice size. These values agree well with the results obtained by fitting the experimental data with the Birch–Murnaghan equation of state, 270–319 GPa.

From the optimized O–Ru bond lengths, we found that the value of u ($u \equiv d_{Ru-O}/\sqrt{2}a$) varies over a very small range under high pressure (from 0.3056 for the lattice with a 3% compression to 0.3074 for that with 1% expansion). This value of u agrees with the experimental result, 0.3058. From the calculated effective elastic constants (based on a spring–mass model), the phonon frequencies of the Ru–O stretch (A_{1g}) and rotational B_{lg} modes are 655 cm^{-1} and 180 cm^{-1}, respectively. As shown in figure 3, the calculated phonon frequencies agree with corresponding results obtained from the Raman spectra (645 cm^{-1} for the A_{lg} mode and 165 cm^{-1} for the B_{1g} mode [4]), indicating the validity and accuracy of our first-principles approach for investigations of MO_2 compounds. As also found in Raman scattering observations [4], the phonon frequencies depend strongly on the lattice constants. The frequency of the A_{lg} mode increases monotonically when the lattice is compressed. By contrast, the B_{lg} mode is gradually softened under pressure and its frequency approaches zero when the lattice constant shrinks by 3.6%.

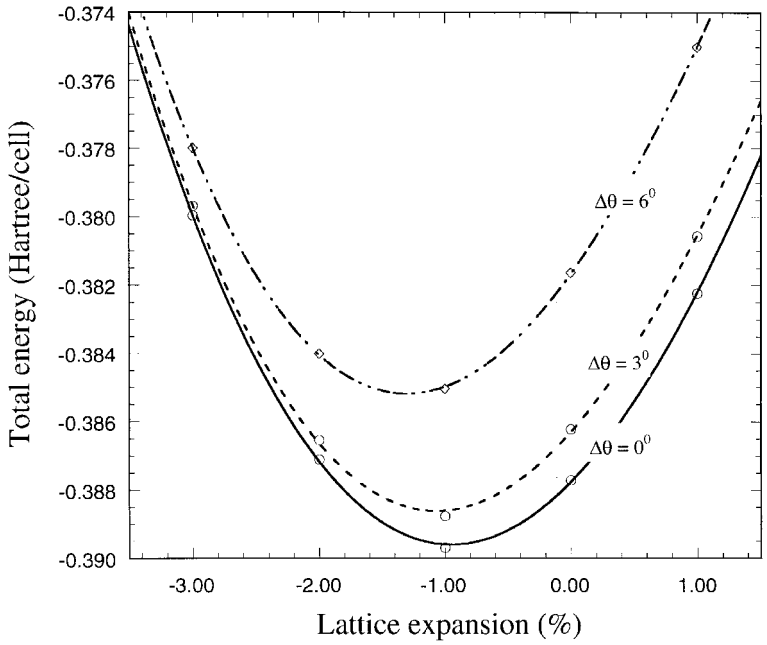

Figure 2. The calculated total energies versus the lattice expansion for three different rotational angles of the RuO_6 octahedra for RuO_2. The $\Delta\theta = 0^\circ$ case corresponds to the rutile structure.

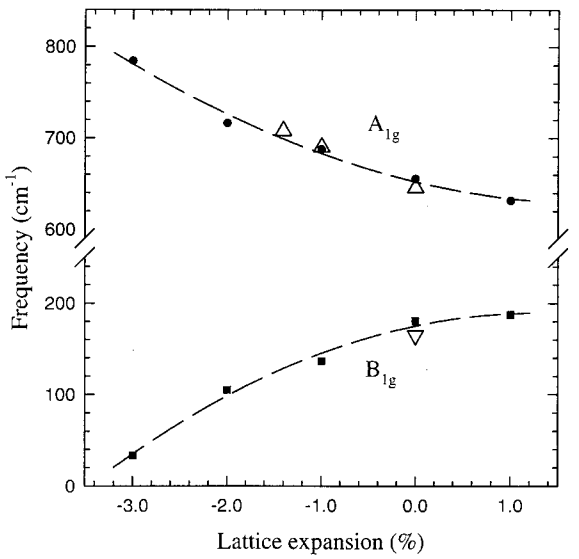

Figure 3. The calculated dependence of the phonon frequencies (A_{1g} and B_{1g} modes) on the lattice expansion for RuO_2. The small solid points are the calculated values; the dashed lines are quadratic fits drawn through these points as a guide to the eye; and the large open triangles are the experimental data converted from reference [4] using the calculated bulk modulus.

To determine the critical pressure for the rutile–$CaCl_2$ phase transition in RuO_2, the total-energy differences, namely, $E_{\theta=3^\circ} - E_{\theta=0^\circ}$ and $E_{\theta=6^\circ} - E_{\theta=0^\circ}$, are plotted in figure 4. For

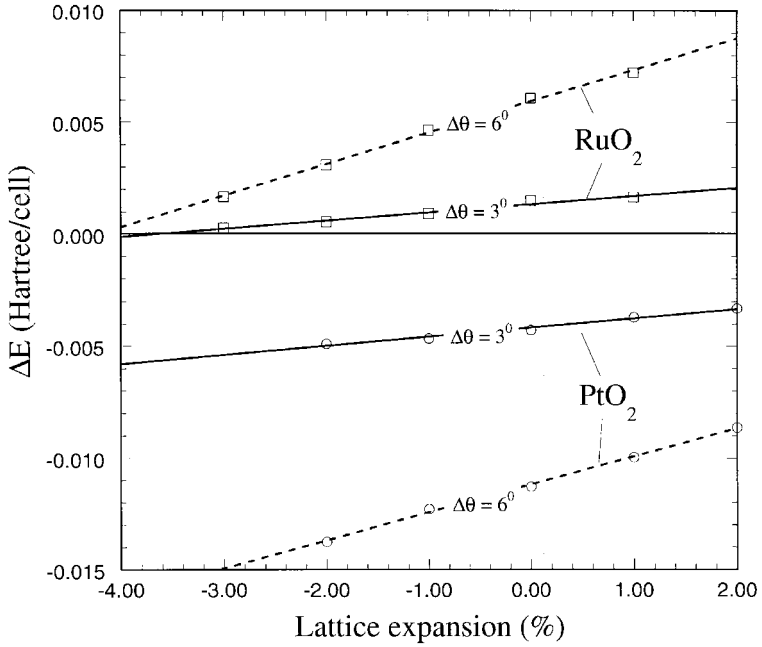

Figure 4. The total-energy differences between rutile and $CaCl_2$-like structures for RuO_2 and β-PtO_2 versus the lattice expansion.

both angles, the total-energy differences decrease almost linearly with the lattice compression. They approach zero when the lattice constant is compressed by 3.5%, at almost the same place where the frequency of the B_{1g} mode becomes zero. From the difference between the critical lattice compressions for $\theta = 6^\circ$ (4.2%) and $\theta = 3^\circ$ (3.6%), we can expect the onset of the rutile-to-$CaCl_2$ phase transition for RuO_2 to occur at a lattice compression of 3–3.5%. From the slope of the total-energy curves in figure 2, this lattice compression requires a critical pressure of 24–27 GPa, a value which is somewhat larger than its experimental counterpart, 11.8 ± 0.3 GPa [3]. There are several factors that may contribute to this discrepancy:

(1) the theoretical results are for a perfect crystal while the experimental samples may be slightly oxygen deficient;
(2) we compress the c-axis together with the lattice size in the xy-plane whereas the length of the c-axis was found to be less sensitive to the pressure [5]; and
(3) we are not allowing for the slight orthorhombic distortion that occurs along with the rotation of the MO_6 octahedra.

The results for PtO_2, as also plotted in figure 4, show a very different behaviour. The rutile structure is much higher in energy than the $CaCl_2$ structure for PtO_2 over the whole range of expansion/compression investigated. In fact, the energy difference between the rutile and $CaCl_2$ structures increases with lattice shrinkage. If we extrapolate along the lines of total-energy differences, the rutile structure can be lower in energy only if the lattice constant expands by about 9–10%. This result is at least qualitatively consistent with the thermal expansion that might occur at the extrapolated transition temperature of 1240 K, determined from the Raman data [7]. From the total-energy curves in figures 5 and 6, we find for β-PtO_2 that

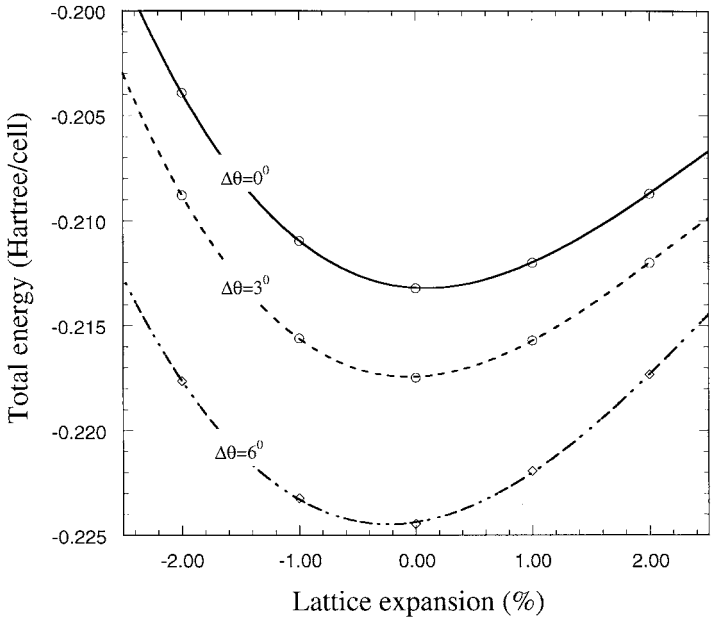

Figure 5. The calculated total energies versus the lattice expansion for three different rotational angles of the PtO_6 octahedra for PtO_2. The $\Delta\theta = 0^\circ$ case corresponds to the rutile structure.

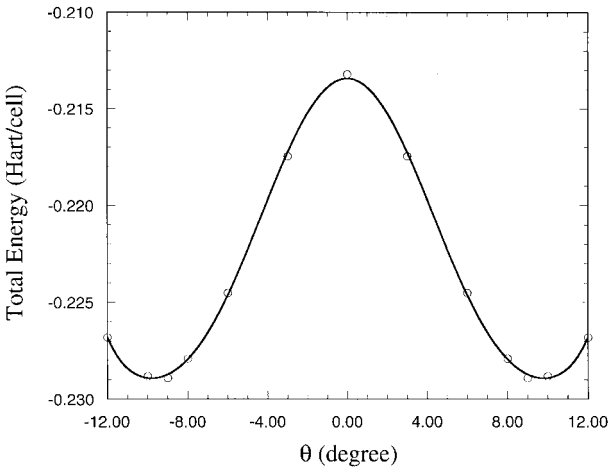

Figure 6. The calculated total energies versus the rotational angle of the PtO_6 octahedra for β-PtO_2 for zero expansion ($a = 4.484$ Å and $c = 3.136$ Å).

(1) the equilibrium lattice constants are $a = 4.509$ Å and $c = 3.112$ Å;
(2) the bulk modulus is 265 GPa; and
(3) the angle of the O–Pt–O bond is 9.4° away from the diagonal direction.

These results agree well with corresponding experimental results [11]. From the curvature of the total energy versus angle in figure 6, the calculated frequency of the Raman mode ω_1 is 279 cm^{-1}, compared with the experimental value of 205 cm^{-1}. The agreement between the

experiment and these calculations for both the ω_1-frequency and the O–Pt–O angle away from the diagonal are strong indications of the validity of our simplifying assumptions regarding a fixed c/a ratio and no orthorhombic distortion.

4. Discussion

We now address the question of why β-PtO_2 adopts the $CaCl_2$ structure while RuO_2 adopts the rutile structure under ambient conditions. From the curves for the densities of states (DOS) in figures 7 and 8, we found that these two crystals differ significantly in their electronic structures. A strong hybridization between Pt 5d and O 2p states occurs over a wide energy range. By contrast, the narrower Ru 4d band separates well from the O 2p band and thus RuO_2 can be considered as an ionic crystal. Significantly, as shown in figure 7, there is a pronounced peak

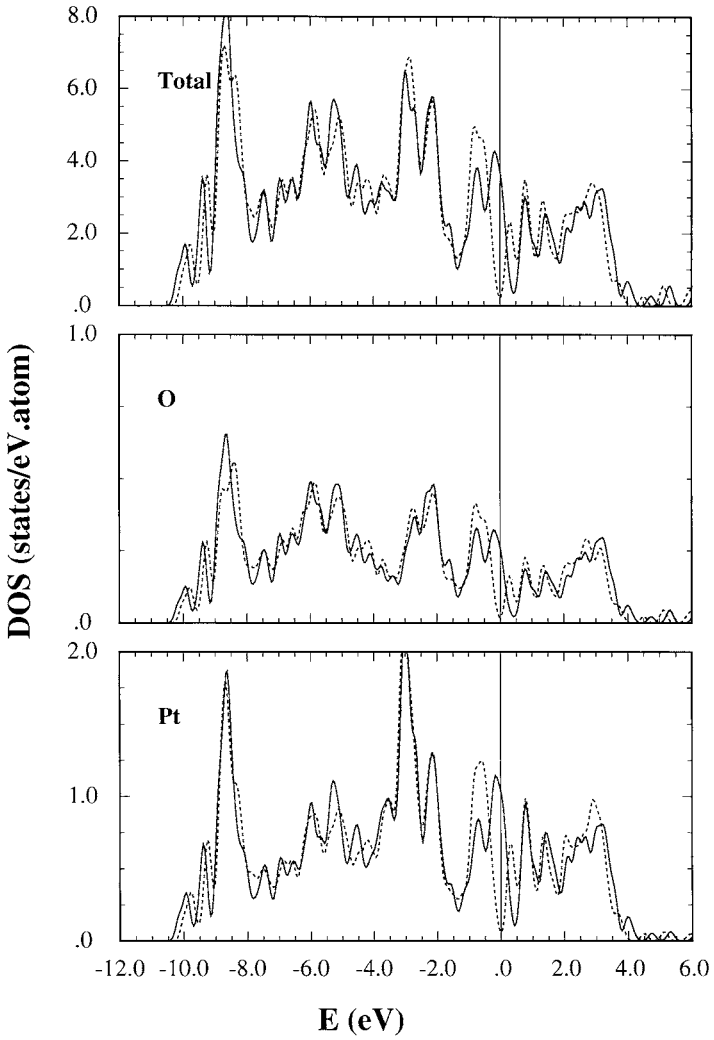

Figure 7. The atom-projected density of states for PtO_2 in the rutile (solid lines) and $CaCl_2$ (dashed lines, $\Delta\theta = 6^\circ$) structures.

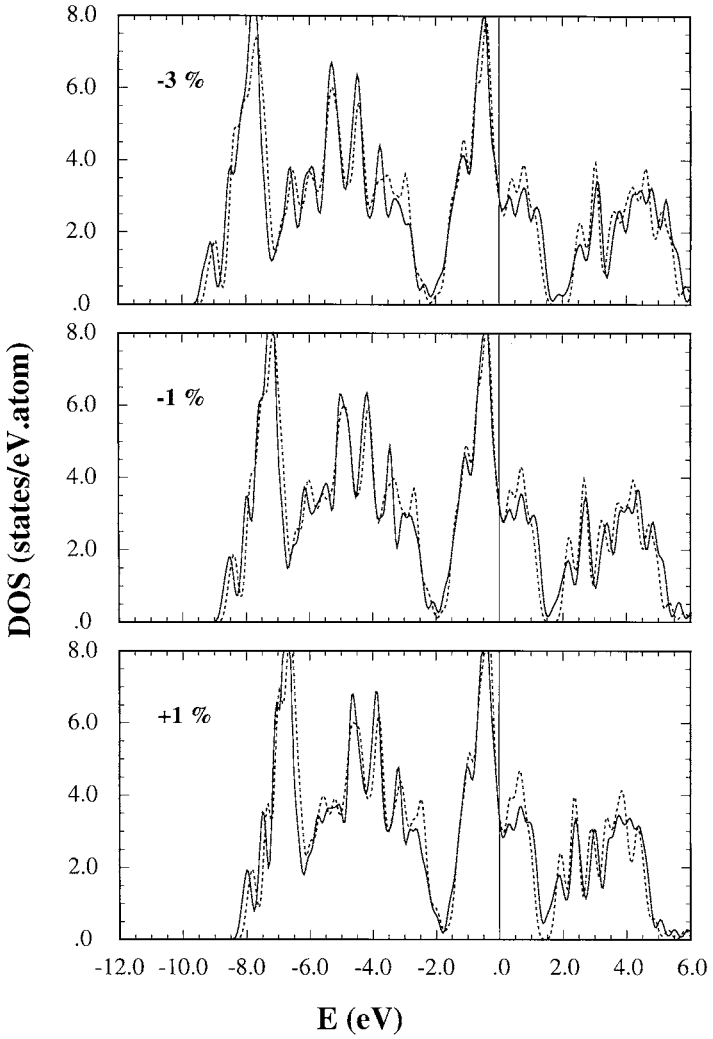

Figure 8. The calculated total density of states for RuO_2 in the rutile (solid lines) and $CaCl_2$ (dashed lines, $\Delta\theta = 6^\circ$) structures for three different lattice expansions.

lying right at the Fermi level for PtO_2 in the rutile structure (solid lines). The charge density at E_F (from states within ± 0.25 eV around the Fermi level) in figure 9(a) indicate that this peak is from the Pt d_{xy} and O p_{x-y} anti-bonding states. As is known, a large value of the DOS at E_F usually causes instabilities and leads to a phase transition. Indeed, this peak is removed and a pseudo-gap is opened at the Fermi level when the $CaCl_2$ structure is adopted (dashed lines in figure 7), mainly through the re-hybridization between the O p_{x-y} states. As seen in figure 9(a), the O p_{x-y} lobes in adjacent cells can form σ-bonds in the $CaCl_2$ phase, which thus stabilizes the β-PtO_2 structure. This opening of a gap at the Fermi level also indicates that the ω_1-mode will strongly modulate the optical properties, which means that this mode will have a large Raman cross section. Confirming this prediction, the ω_1-mode of β-PtO_2 was found to be the strongest line in the spectrum [7]. In contrast, the corresponding mode is the weakest line in the spectrum in similar rutile-structured dioxides, RuO_2 and IrO_2 [4, 12].

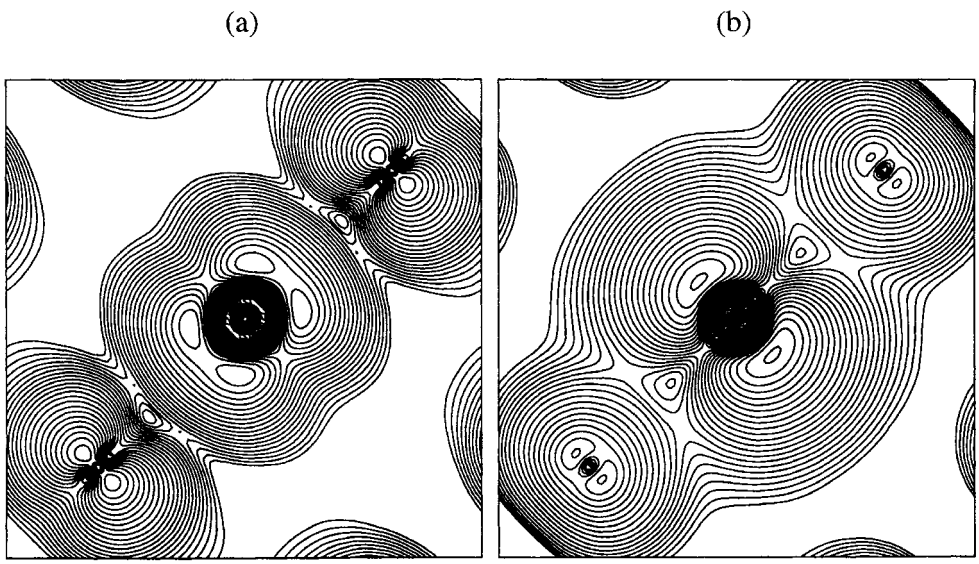

Figure 9. The charge density at E_F (contributed from states within ± 0.25 eV around the Fermi level) for (a) PtO_2 and (b) RuO_2 in the rutile structure. Contours start from 5×10^{-4} e au^{-3} and increase successively by a factor of $10^{1/10}$.

The profiles of the DOS curves of RuO_2 [13], however, are insensitive to both the change of the lattice size and the rotation of the O–Ru–O bonds in figure 8 (the bandwidth increases with the lattice compression). Its charge density at E_F in figure 9(b), because the Ru 4d band has fewer electrons and stronger localization, is dominated by the Ru states (within ± 0.25 eV, there are 0.67 electrons in each Ru sphere, but only 0.08 electrons in each O sphere). No significant O–O re-hybridization occurs in RuO_2 (it does in PtO_2, where the weight of O contributions to the states at E_F is more than double). Therefore, the pressure-induced rutile–$CaCl_2$ phase transition in RuO_2 appears not to be due to the change of valence interaction, but to be determined by the electrostatic interactions. In fact, the interatomic distances are shortened under high pressure which results in a strong repulsion between O atom and O atom along the diagonal direction [14]. The repulsive stress is significantly reduced through the rutile–$CaCl_2$ phase transition, which preserves the Ru–O bonds but lengthens the O–O bonds between adjacent unit cells ($d_{O-O} = a\sqrt{2(1 + 4u^2 - 4u\cos\theta)}$) and thus reduces the free energy. On the other hand, the electrostatic interaction always favours the rutile structure. Indeed, we found that the Madelung energy in the $CaCl_2$ structure ($\alpha = 4.8255$ for $\Delta\theta = 6^\circ$ and $u = 0.306$) is much higher than that in the rutile structure ($\alpha = 4.8393$ for $\Delta\theta = 0^\circ$ and $u = 0.306$). Therefore, the phase stability of RuO_2 is mainly determined by a competition between the intra-cell Ru–O and O–O repulsions and the inter-cell anion–anion interactions.

5. Conclusions

In conclusion, the pressure-induced rutile–$CaCl_2$ phase transition of RuO_2 can be reproduced in our FLAPW calculations. The competition between the interatomic repulsion (O–O and Ru–O) and the electrostatic interaction (the Madelung part) is found to play an essential role in the phase stability. On the other hand, a strong hybridization between O 2p and Pt 5d

determines the phase stability of β-PtO_2 for which the rutile–$CaCl_2$ phase transition opens a pseudo-gap at the Fermi level and thus reduces the DOS value to almost zero.

Acknowledgments

We thank Dr V Gavrilenko for providing the Madelung constants and Dr K C Hass for a critical reading of the manuscript. This work was supported by the US Department of Energy, Office of Basic Energy Sciences, Division of Chemical Sciences (grant No DE-FG03-99ER14948) and by computing grants at NERSC. RW thanks Parson's Foundation for support in upgrading computer facilities at CSUN.

References

[1] Glassford K M and Chelikowsky J R 1994 *Phys. Rev.* B **49** 7107
[2] Krasovska O V, Krasovskii E E and Antonov V N 1995 *Phys. Rev.* B **52** 11 825
[3] Zheng J P and Jow T R 1995 *J. Electrochem. Soc.* **142** L6
[4] Rosenblum S S, Weber W H and Chamberland B L 1997 *Phys. Rev.* B **56** 529
[5] Haines J and Léger J M 1993 *Phys. Rev.* B **48** 13 344
[6] Haines J and Léger J M 1997 *Phys. Rev.* B **55** 11 144
Haines J, Léger J M and Schulte O 1996 *J. Phys.: Condens. Matter* **8** 1631
Haines J, Léger J M and Hoyau S 1995 *J. Phys. Chem. Solids* **56** 965
[7] Weber W H, Graham G W and McBride J R 1990 *Phys. Rev.* B **42** 10 969
[8] Karki B B, Warren M C, Stixrude L, Ackland G J and Crain J 1997 *Phys. Rev.* B **55** 3465
[9] Lee C and Gonze X 1997 *Phys. Rev.* B **56** 7321
[10] Wimmer E, Krakauer H, Weinert M and Freeman A J 1981 *Phys. Rev.* B **24** 864
Weinert M, Wimmer E and Freeman A J 1982 *Phys. Rev.* B **26** 4571 and references therein
[11] The lattice constants of β-PtO_2 based on the refinement by
Range K-J *et al* 1987 *Mater. Res. Bull.* **22** 1541
are $a = 4.4839$ Å, $b = 4.5385$ Å and $c = 3.1360$ Å with the O–Pt–O bond 8.1° away from the diagonal direction.
[12] Huang Y S, Lin S S, Huang C R, Lee M C, Dann T E and Chien F Z 1989 *Solid State Commun.* **70** 517
[13] The profile of the DOS for RuO_2 here is close to the previous results obtained with other approximate methods such as the LMTO one:
Xu J H, Jarlborg T and Freeman A J 1989 *Phys. Rev.* B **40** 7939
and that of pseudopotentials:
Glassford K M and Chelikowsky J R 1993 *Phys. Rev.* B **47** 1732
and also the LAPW one:
Krasovska O V, Krasovskii E E and Antonov V N 1995 *Phys. Rev.* B **52** 11 825
[14] The O–O distance along the diagonal direction is only 2.42 Å, which is far smaller than the equilibrium O–O bond length (2.98 Å) given by the Dashevsky potential ($V(r) = -354\,r^{-6} + 96\,500\,e^{-4.333r}$ kcal mol^{-1}); see for example
Hyde B G 1987 *Z. Kristallogr.* **179** 205